Mean-Square Optical Anisotropy of Oligo- and Poly(α-methylstyrene)s in Dilute Solution

Hideaki Kojo, Masashi Osa, Takenao Yoshizaki, and Hiromi Yamakawa*

Department of Polymer Chemistry, Kyoto University, Kyoto 606-8501, Japan

Received April 24, 2003; Revised Manuscript Received June 11, 2003

ABSTRACT: The mean-square optical anisotropy $\langle\Gamma^2\rangle$ was determined from anisotropic light scattering measurements for 10 samples of atactic oligo- and poly(α-methylstyrene)s (a-PαMS) with the fraction of racemic diads $f_r = 0.72$ in the range of weight-average degree of polymerization x_w from 2 to 67.1 in cyclohexane at 30.5 °C (Θ). A comparison is made of the present data with the helical wormlike (HW) chain theory with the values of the model parameters previously determined from the mean-square radius of gyration and with those of the local polarizability tensor $\boldsymbol{\alpha}_0$ per repeat unit properly assigned on the basis of the bond and group polarizabilities. The HW theory value of $\langle\Gamma^2\rangle/x_w$ in the limit of $x_w \to \infty$ is found to be somewhat larger than the experimental one. It is then shown that if $\boldsymbol{\alpha}_0$ is replaced by $0.9_0\boldsymbol{\alpha}_0$, the HW theory may reproduce quantitatively the experimental results for all the samples except those with $x_w \leq 4$ for which effects of chain ends become appreciable. A comparison is also made of the present results for a-PαMS with previous ones for atactic polystyrene ($f_r = 0.59$), atactic poly(methyl methacrylate) (a-PMMA) ($f_r = 0.79$), isotactic PMMA ($f_r \simeq 0.01$), and poly(*n*-hexyl isocyanate), and the behavior of $\langle\Gamma^2\rangle$ is shown to depend remarkably on chain stiffness and local chain conformation.

Introduction

In a series of experimental studies of dilute solution properties of atactic oligo- and poly(α-methylstyrene)s (a-PαMS) with the fraction of racemic diads $f_r = 0.72$ in the unperturbed Θ state,[1−3] we have analyzed data for the mean-square radius of gyration[1] $\langle S^2\rangle_\Theta$, scattering function[2] $P_s(k)$, intrinsic viscosity[3] $[\eta]_\Theta$, and translational diffusion coefficient[3] D_Θ on the basis of the helical wormlike (HW) chain model.[4] From the values of the HW model parameters determined from them, it has been concluded that the a-PαMS chain has rather large chain stiffness and strong helical nature like the atactic poly(methyl methacrylate) (a-PMMA) chain with $f_r = 0.79$.[4,5] We note that by the term "helical nature", we mean that the chain tends to retain large and clearly distinguishable helical portions in dilute solution.[4] As is well-known,[4,6] the mean-square optical anisotropy $\langle\Gamma^2\rangle$ determined from anisotropic light scattering (LS) measurements may also provide useful information about chain stiffness and local chain conformation. Thus, in the present study, we proceed to determine $\langle\Gamma^2\rangle$ as a function of molecular weight M (or degree of polymerization x) for a-PαMS in the Θ state, i.e., in cyclohexane at 30.5 °C.[1]

We have already made experimental investigations of $\langle\Gamma^2\rangle$ for atactic polystyrene (a-PS)[4,7,8] with $f_r = 0.59$, a-PMMA with $f_r = 0.79$,[4,8] and isotactic (i-) PMMA[4,9] with $f_r \simeq 0.01$ as typical examples of flexible polymers and also for poly(*n*-hexyl isocyanate) (PHIC)[10] as that of semiflexible polymers. In all cases, it has been shown that the behavior of $\langle\Gamma^2\rangle$ as a function of x may be well explained by the corresponding HW theory[4,11] or the theory[4,12,13] based on the Kratky−Porod (KP) wormlike chain[4,14] with the values of the model parameters determined from $\langle S^2\rangle_\Theta$ along with those of the local polarizability tensor reasonably assigned. The main purpose of this paper is therefore to examine whether the behavior of $\langle\Gamma^2\rangle$ for a-PαMS may be explained by the HW theory with the values of the model parameters previously determined from $\langle S^2\rangle_\Theta$.[1]

The quantity $\langle\Gamma^2\rangle$ of a-PαMS itself is of great interest to us also for the following reason. About 30 years ago, Utiyama and Tsunashima[15,16] determined the effective bond anisotropy Λ, which is proportional to $(\langle\Gamma^2\rangle/x)^{1/2}$, from anisotropic LS measurements for a-PαMS with $f_r = 0.68$ in *trans*-decalin[15,16] and in cyclohexane,[16] both near Θ, in the range of weight-average molecular weight M_w from 3.76×10^5 to 6.85×10^6, and showed that Λ increases with increasing M_w even for such large M_w. None of the existent theories can explain this behavior; all of them predict that it (or $\langle\Gamma^2\rangle/x$) becomes a constant independent of M for large M. A careful determination of the dependence of $\langle\Gamma^2\rangle/x$ on x (or M) is therefore required for the present study. Thus, we carry out anisotropic LS measurements to determine $\langle\Gamma^2\rangle$ accurately by using a Fabry−Perot (FP) interferometer with a set of a polarizer and an analyzer having very small extinction ratios, as done in previous studies.[8,9] The use of these facilities enables us to eliminate possible effects of collision-induced polarizabilities[6] and the polarized component of the scattered intensity, respectively.

Experimental Section

Materials. All the a-PαMS samples used in this work are the same as those used in the previous studies of $\langle S^2\rangle_\Theta$,[1] $P_s(k)$,[2] $[\eta]_\Theta$,[3] and D_Θ,[3] i.e., fractions separated by preparative gel permeation chromatography (GPC) or fractional precipitation from the original samples prepared by living anionic polymerization.[1,17] We note that the initiating chain end of each polymerized sample is a *sec*-butyl group and the other end is a hydrogen atom.

The values of M_w determined from ^{1}H and ^{13}C NMR spectra by analytical GPC or from LS measurements (in cyclohexane at 30.5 °C), the weight-average degree of polymerization x_w estimated from M_w, the ratio of M_w to the number-average molecular weight M_n determined by analytical GPC,[1,3] and f_r determined from ^{1}H and ^{13}C NMR spectra[1,17] are given in Table 1. Although f_r of the samples OAMS4−OAMS10 could not be determined because of the complexity of their ^{1}H NMR spectra, they may be regarded as having almost the same value of f_r ($0.71 \lesssim f_r \lesssim 0.73$) as OAMS3 or OASM13 with $M_w = 1.60 \times$

10.1021/ma034536r CCC: $25.00
Published on Web 07/29/2003

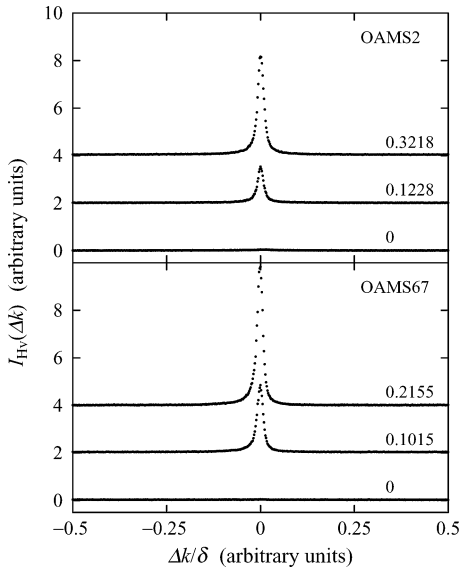

Figure 1. Plots of $I_{Hv}(\Delta k)$ against $\Delta k/\delta$ for a-PαMS samples OAMS2 and OAMS67 in cyclohexane at 30.5 °C (Θ) at the indicated values of c (in g/cm^3). For each sample, the data points for the solution at $c = 0$ are those for the pure solvent, and those for the solutions at the medium and highest c are shifted upward by 2 and 4, respectively.

Table 1. Values of M_w, x_w, M_w/M_n, and f_r for Atactic Oligo- and Poly(α-methylstyrene)s

sample	M_w	x_w	M_w/M_n	f_r
OAMS2	2.94×10^2	2	1	0.56
OAMS3	4.12×10^2	3	1	0.73
OAMS4	5.30×10^2	4	<1.01	
OAMS5	6.48×10^2	5	<1.01	
OAMS6	7.66×10^2	6	<1.01	
OAMS8	1.04×10^3	8.29	1.01	
OAMS10	1.27×10^3	10.3	1.01	
OAMS19	2.27×10^3	18.7	1.07	0.72
OAMS38	4.57×10^3	38.2	1.07	0.72
OAMS67	7.97×10^3	67.1	1.04	0.72

10^3 (which is not used in this work), since the samples OAMS3−OAMS13 are fractions from one original sample.[17] As seen from the values of f_r, all the samples except OAMS2 have the fixed stereochemical composition $f_r = 0.72 \pm 0.01$. As previously[3] mentioned, the difference in f_r between the sample OAMS2 and the others may be regarded as arising from that in reaction mechanism; i.e., f_r of the former is determined by the termination reaction with methanol, while those of the latter are determined (mainly) by the propagation reaction. As seen from the values of M_w/M_n, all the samples are very narrow in molecular weight distribution.

The solvent cyclohexane used for anisotropic LS measurements was purified according to a standard procedure.

Anisotropic Light Scattering. The photometer used for all anisotropic LS measurements is the same as that used in the previous studies of a- and i-PMMAs,[8,9] i.e., a Brookhaven Instruments model BI-200SM goniometer with a minor modification of its light source part and with a detector alignment previously assembled to incorporate an FP interferometer in it. It has been described in detail in the previous paper,[8] and therefore, we here give only its short sketch (see Figure 1 of ref 8).

Vertically polarized light of wavelength 488 nm from a Spectra-Physics model 2020 argon ion laser equipped with a model 583 temperature-stabilized etalon for single-frequency-mode operation was used as a light source. It was made highly vertically (v) polarized by passing it through a Glan−Thompson (GT) prism with an extinction ratio smaller than 10^{-5}. The scattered light was measured at a scattering angle of 90°. Its horizontal (H) component, i.e., the depolarized (Hv) component, which was extracted from the total scattered intensity by the use of the same GT prism as above, was analyzed with a Burleigh Instruments model RC-110 FP interferometer equipped with a model RC-670 pair of plane mirrors with flatness of $\lambda/200$ and a reflectivity of 97.5%. The intensity of the Hv component filtered through the FP interferometer was measured by an EMI9893B/350 photomultiplier (PM) tube. As in the previous studies,[8,9] we used a pinhole of diameter 100 μm as a spatial filter, which was placed between the interferometer and the PM tube. All the measurements were carried out in cyclohexane at 30.5 °C (Θ) by the single-passing operation of the interferometer.

The most concentrated solution of each sample was prepared gravimetrically and made homogeneous by continuous stirring for ca. 1 day at ca. 50 °C. These solutions and the solvent were optically purified by filtration through a Teflon membrane of pore size 0.1 μm. The solutions of lower concentrations were obtained by successive dilution. The weight concentrations of the test solutions were converted to the solute mass concentrations c (in g/cm^3) by the use of the densities of the solutions.

Before and after each measurement on the solution or solvent, the spectrum of the Hv component scattered from pure benzene sealed in a Pyrex nuclear magnetic resonance tube of outer diameter 10 mm, which we used as a working standard (WS), was measured without a narrow band-pass filter in order to monitor any possible changes in the photometer system, as done in the previous static measurements.[8,9] Before every set of three measurements on pure benzene, on the solution or solvent, and again on benzene, the FP interferometer was tuned to obtain the highest finesse. The value of the finesse was 40−50 just after the tuning and usually decreased to 30−40 after the set of measurements, which took ca. 1 h. The free spectral range (FSR) was adjusted to be 5−50 cm^{-1}.

As an example, Figure l shows FP spectra of the depolarized component $I_{Hv}(\Delta k)$ of the scattered intensity as a function of the wavenumber difference Δk between the incident and scattered light divided by the value δ of FSR for solutions of OAMS2 in cyclohexane at $c = 0.3218$ and 0.1228 g/cm^3 and of OAMS67 in cyclohexane at $c = 0.2155$ and 0.1015 g/cm^3, and also for the solvent cyclohexane ($c = 0$), all at 30.5 °C. All the values of I_{Hv} have been reduced by the total intensity of the Hv component determined for the WS from the measurements mentioned above. For each sample, the data points for the solutions at the medium and highest c are shifted upward by 2 and 4, respectively. It is seen that for each sample, the peak at $\Delta k = 0$ in the spectrum becomes small as c is decreased, and nearly vanishes for the pure solvent, indicating that the peak arises only from the optical anisotropy intrinsic to a-PαMS, the intrinsic optical anisotropy of cyclohexane being vanishingly small, as was expected. Possible effects of collision-induced polarizabilities on I_{Hv} for the solutions and solvent may be considered to contribute to the low flat base parts of the spectra since their peak widths are in general much broader than δ.[6]

As in the cases of a- and i-PMMAs previously[8,9] studied, we may evaluate the excess Hv component $\Delta I_{Hv}(\Delta k)$ of the scattered intensity from

$$\Delta I_{Hv}(\Delta k) = I_{Hv,soln}(\Delta k) - \phi\, I_{Hv,solv}(\Delta k) \qquad (1)$$

with the values of $I_{Hv}(\Delta k)$ for the solution and solvent, where ϕ is the volume fraction of the solvent.

As in the previous studies,[8,9] the total intensity $\Delta I_{Hv,mol}$ of the intrinsic molecular part of the excess Hv component was evaluated by numerical integration of the observed quantity $\Delta I_{Hv}(\Delta k) - I_{base}$ over Δk in the range of one FSR, where I_{base} is the intensity of the flat base part of the FP spectrum due to the effect of collision-induced polarizabilities.

Now the intrinsic molecular excess Hv component $\Delta R_{Hv,mol}$ of the reduced intensity may be calculated from

$$\Delta R_{Hv,mol} = \frac{\tilde{n}^2\, \phi_A}{T_{max}} \Delta I_{Hv,mol} \qquad (2)$$

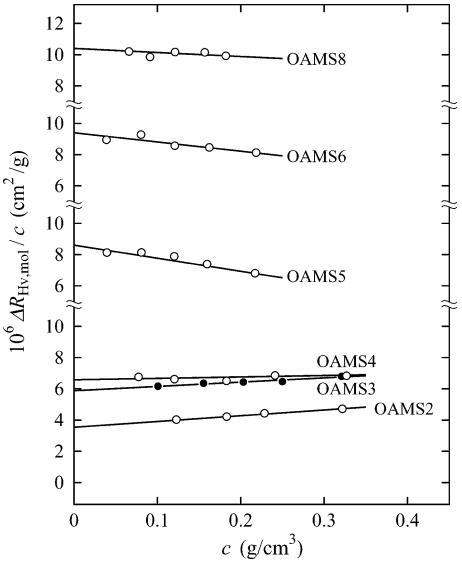

Figure 2. Plots of $\Delta R_{\mathrm{Hv,mol}}/c$ against c for a-PαMS samples OAMS2 through OAMS8 in cyclohexane at 30.5 °C (Θ).

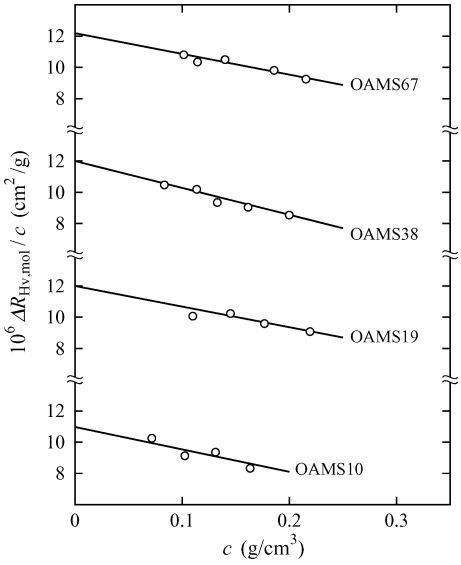

Figure 3. Plots of $\Delta R_{\mathrm{Hv,mol}}/c$ against c for a-PαMS samples OAMS10 through OAMS67 in cyclohexane at 30.5 °C (Θ).

with the value of $\Delta I_{\mathrm{Hv,mol}}$ determined above, where $\tilde{n}$ is the refractive index of the solvent, $T_{\max}$ is the maximum (or peak) transmittance of the narrow band-pass filter, and ϕ_{A} is the apparatus constant depending on the photometer used. In eq 2, the $\tilde{n}^2$ correction of Hermans and Levinson[18] has been applied, and also a correction to $\Delta I_{\mathrm{Hv,mol}}$ for the absorption by the narrow band-pass filter has been simply made by the factor $1/T_{\max}$ since the width of the resultant spectrum of the excess scattered intensity (as shown in Figure 1) is very narrow compared to the full width at half-maximum of the filter. The value of ϕ_{A} is usually determined so that the value of the Hv component $\tilde{n}_{(\mathrm{benzene})}{}^2\phi_{\mathrm{A}}I_{\mathrm{Hv(benzene)}}$ of the reduced intensity of the light scattered from pure benzene measured at a scattering angle of 90 ° by the use of the photometer coincides with the value of the Hv component $R_{\mathrm{Hv(benzene)}}$ of the reduced intensity absolutely determined, where $I_{\mathrm{Hv(benzene)}}$ is the (total) intensity of the Hv component measured under the same conditions of the apparatus (including the sample cell) as in the case of the measurements on the test solutions but without the narrow band-pass filter. Then ϕ_{A} may be obtained from

$$\phi_{\mathrm{A}} = R_{\mathrm{Hv(benzene)}}/\tilde{n}_{(\mathrm{benzene})}{}^2 I_{\mathrm{Hv(benzene)}} \tag{3}$$

$R_{\mathrm{Hv(benzene)}}$ is a quantity depending only on pressure, temperature, and the wavelength of the incident light, and therefore must be determined without the narrow band-pass filter, so that the intensity $I_{\mathrm{Hv(benzene)}}$ (relative to the WS) must also be determined without the narrow band-pass filter.

The value of $R_{\mathrm{Hv(benzene)}}$ at 30.5 °C we used is 8.16×10^{-1} cm^{-1}, which had been determined at 25.0 °C in the previous study.[8] We note that $I_{\mathrm{Hv(benzene)}}$ and therefore $R_{\mathrm{Hv(benzene)}}$ are almost independent of temperature in its range from 25.0 to 30.5 °C, as previously[8] mentioned. The values of the refractive index we used for benzene and cyclohexane at 30.5 °C are 1.516 and 1.426, respectively.

Results

Figure 2 shows plots of the ratio of the intrinsic molecular excess Hv component $\Delta R_{\mathrm{Hv,mol}}$ of the reduced intensity to the mass concentration c against c for the samples OAMS2 through OAMS8 in cyclohexane at 30.5 °C (Θ). Figure 3 shows similar plots for the samples OAMS10 through OAMS67 in the same solvent condition. As seen from these figures, the data points for each sample follow a straight line and can be extrapolated to infinite dilution to determine $(\Delta R_{\mathrm{Hv,mol}}/c)_{c=0}$ rather unambiguously, as in the cases of a- and i-PMMAs[8,9] previously studied.

Table 2. Values of $\langle\Gamma^2\rangle/x_{\mathrm{w}}$ for Atactic Oligo- and Poly(α-methylstyrene)s in Cyclohexane at 30.5 °C (Θ)

sample	$\langle\Gamma^2\rangle/x_{\mathrm{w}}$, Å^6
OAMS2	35.$_1$
OAMS3	54.$_5$
OAMS4	58.$_8$
OAMS5	75.$_2$
OAMS6	80.$_9$
OAMS8	88.$_0$
OAMS10	91.$_2$
OAMS19	98.$_2$
OAMS38	96.$_8$
OAMS67	97.$_6$

If the effect of the internal field is taken into account by the use of the Lorentz−Lorenz equation as in the previous studies,[7−10] the mean-square optical anisotropy $\langle\Gamma^2\rangle$ may be calculated from

$$\langle\Gamma^2\rangle = \frac{15\lambda_0{}^4}{16\pi^4}\frac{M}{N_{\mathrm{A}}}\left(\frac{3}{\tilde{n}^2+2}\right)^2\left(\frac{\Delta R_{\mathrm{Hv,mol}}}{c}\right)_{c=0} \tag{4}$$

with the observed value of $(\Delta R_{\mathrm{Hv,mol}}/c)_{c=0}$ determined above, where λ_0 is the wavelength of the incident light in a vacuum and is equal to 488 nm, N_{A} is the Avogadro constant, and $\tilde{n}$ is the refractive index of the solvent. We have already discussed the adoption of the internal field correction of the second power type in eq 4 in the previous study.[8] As mentioned there, this adoption is only a matter of convenience for a comparison of the present results with the previous ones and also with literature data and may be considered to be sufficient for the present main purpose that we analyze the dependence of $\langle\Gamma^2\rangle/x_{\mathrm{w}}$ on x_{w} on the basis of the HW chain model.

The values of $\langle\Gamma^2\rangle/x_{\mathrm{w}}$ for all the a-PαMS samples in cyclohexane at 30.5 °C (Θ) calculated from eq 4 with the values $(\Delta R_{\mathrm{Hv,mol}}/c)_{c=0}$ determined above are given in Table 2. Figure 4 shows plots of $\langle\Gamma^2\rangle/x_{\mathrm{w}}$ so obtained against log x_{w}. The solid curve connects smoothly the data points. It is seen that as x_{w} is increased, $\langle\Gamma^2\rangle/x_{\mathrm{w}}$ (the mean-square optical anisotropy per repeat unit) first increases monotonically for $x_{\mathrm{w}} \lesssim 10$ and then

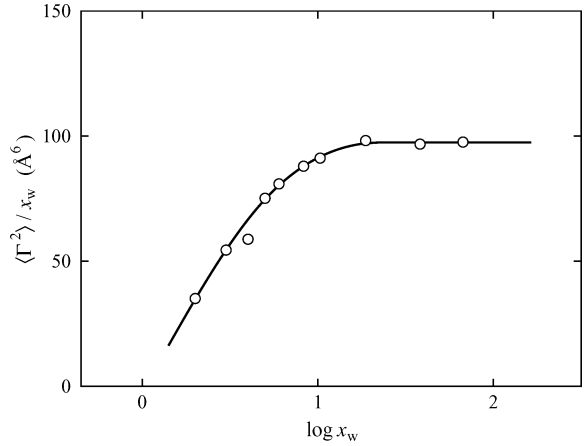

Figure 4. Plots of $\langle\Gamma^2\rangle/x_w$ against logx_w for a-PαMS in cyclohexane at 30.5 °C (Θ). The solid curve connects smoothly the data points.

approaches a constant asymptotic value of ca. 100 Å^6 for $x_w \gtrsim 10$.

It is pertinent to refer here to the data by Utiyama and Tsunashima[15,16] for a-PαMS with $f_r = 0.68$ in *trans*-decalin and in cyclohexane, both near Θ, mentioned in the Introduction. They have used the optical anisotropy parameter[19] δ or the effective bond anisotropy[15,16] Λ defined by $\Lambda = (M\delta)^{1/2}$ to present their experimental results of anisotropic LS measurements. The values of δ or Λ have been determined by the use of the relation[19] $(\Delta R_{Hv,mol}/2Kc)_{c=0} = 3\delta M$ for the Gaussian chain model with the observed values of $(\Delta R_{Hv,mol}/c)_{c=0}$, where K is the optical constant. From their result in cyclohexane at 34.2−34.6 °C (near their Θ equal to 34.9 °C)[16] that Λ increases from 7.1 to 18.3 g$^{1/2}$/mol$^{1/2}$ as M_w is increased from 3.76×10^5 to 6.85×10^6, it can be shown that $\langle\Gamma^2\rangle/x_w$ increases from 890 to 6000 Å^6 as M_w is increased in this range of M_w, where we have assumed the value 0.206 cm^3/g of the refractive index increment $\partial n/\partial c$ in K estimated in cyclohexane at 34.5 °C from the experimental relation, eq 1 of ref 1. As for their result in *trans*-decalin,[15,16] we do not discuss it in detail since there is no available value of $\partial n/\partial c$ in *trans*-decalin, but only note that it is similar to that in cyclohexane. Besides the fact that the behavior of their experimental data is inconsistent with all the existent theories, as mentioned in the Introduction, the values of $\langle\Gamma^2\rangle/x_w$ themselves are 1 or 2 orders of magnitude larger than the above-mentioned asymptotic value of $\langle\Gamma^2\rangle/x_w$ determined in the present study. As shown in the next section, the present asymptotic value is of reasonable order, considering the polarizability of the repeat unit of PαMS. In general, the ratio of the excess polarized component of the scattered intensity to the excess depolarized (Hv) one becomes extremely large with increasing M (or x), the latter being independent of M for large M. Thus, it is plausible to consider that the leak of the former component may possibly lead to such an anomaly in their data.

Discussion

Local Polarizability Tensor. Before proceeding to make a comparison of the present experimental results with the corresponding theory[4,11] on the basis of the HW chain model, we must first assign a proper local polarizability tensor $\boldsymbol{\alpha}$ per unit contour length to the chain. For this purpose, it is necessary to assign a localized Cartesian coordinate system (ξ,η,ζ) affixed to the HW chain to the repeat unit [$CH_2-C^\alpha(CH_3)(C_6H_5)-CH_2$] of the PαMS chain. The procedure of this assignment has already been established for both i- and syndiotactic (s-) PαMS chains in a previous analysis[20] of the rotational isomeric state model[21] data for the angular correlation functions, as depicted in Figure 5. That is, for both i- and s-PαMS chains and therefore also for the a-PαMS chain, the ζ axis is taken along a line passing through the two successive methylene C atoms, the ξ axis is in the plane of the two successive bond vectors $\mathbf{l}_{j-1}$ (C−C$^\alpha$ bond) and $\mathbf{l}_j$ (C$^\alpha$−C bond) with its positive direction chosen at an acute angle with the bond $\mathbf{l}_j$, and the η axis completes the right-handed system. We note that in the figure, the bonds $\mathbf{l}_{j-1}$ and $\mathbf{l}_j$ are *d*- and *l*-chiral, respectively, following the new Flory convention[22] for describing stereochemical configurations of asymmetric chains.

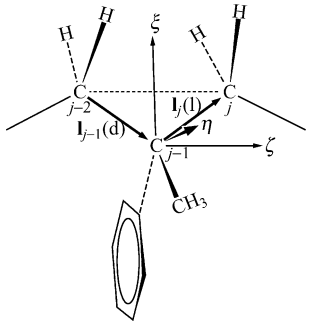

Figure 5. Localized Cartesian coordinate system assigned to the PαMS chain (see the text).

Since the value of f_r of the present a-PαMS samples is rather close to unity, we adopt the polarizability tensor $\boldsymbol{\alpha}_0$ of the repeat unit of the s-PαMS chain as that of the former, for simplicity, as in the previous study of a-PMMA.[8] If we assume the additivity of the bond and group polarizabilities, $\boldsymbol{\alpha}_0$ may be written as a sum of the contribution from the center part [C−C$^\alpha$(CH$_3$)-(C$_6$H$_5$)−C] and one half of the contribution from the CH$_2$ groups on both sides. Strictly speaking, $\boldsymbol{\alpha}_0$ depends on the bond rotation angles around the bonds $\mathbf{l}_{j-1}$ and $\mathbf{l}_j$, so that the $\boldsymbol{\alpha}_0$ averaged over the angles should be used. Because of the predominance of the *tt* conformation in the s-PαMS chain, however, we may use the values of the components of $\boldsymbol{\alpha}_0$ for the *all-trans* conformation, for simplicity, as in the previous study of a-PMMA.[8] By the use of the literature values of the bond and rotational angles[23] and of the bond polarizabilities[6,24,25] for C−C and C−H and the group polarizability[25] for C−C$_6$H$_5$, which have been corrected by multiplying them by the common factor $\gamma = (1.94)^{1/2}$,[8] the (traceless) $\boldsymbol{\alpha}_0$ for the repeat unit with the pair of successive bond chiralities *dl* as shown in Figure 5 may then be given by

$$\boldsymbol{\alpha}_0 = \begin{pmatrix} 1.40 & 1.58 & 0 \\ 1.58 & 2.47 & 0 \\ 0 & 0 & -3.87 \end{pmatrix} (\text{Å}^3) \qquad (5)$$

In the above evaluation of $\boldsymbol{\alpha}_0$, we have assumed that the plane of the phenyl group is perpendicular to the plane of bonds $\mathbf{l}_{j-1}$ and $\mathbf{l}_j$ in the main chain. For the repeat unit with the pair of successive bond chiralities *ld*, $\boldsymbol{\alpha}_0$ is given by eq 5 with both $\xi\eta$ and $\eta\xi$ components being −1.58 in place of 1.58.

In the s-PαMS chain, the pair of successive bond chiralities of the repeat unit and therefore the sign of

the $\xi\eta$ and $\eta\xi$ components change alternately. Thus, the values of $\boldsymbol{\alpha}_0$ obtained above cannot be adopted for $\boldsymbol{\alpha}$ as it stands, since the $\boldsymbol{\alpha}$ to be attached to the HW chain must be constant. In light scattering (with $\lambda_0 = 488$ nm), the fluctuation in the local polarizability tensor on the length scales of the repeat unit is immaterial, and it is sufficient to use the one averaged on somewhat longer length scales. We may then use $\boldsymbol{\alpha}_0$ with vanishing off-diagonal components, i.e.,

$$\boldsymbol{\alpha}_0 = \mathrm{diag}(1.40,\ 2.47,\ -3.87)\ (\text{Å}^3) \tag{6}$$

The tensor $\boldsymbol{\alpha}$ may be calculated from

$$\boldsymbol{\alpha} = (M_L/M_0)\boldsymbol{\alpha}_0 \tag{7}$$

with $\boldsymbol{\alpha}_0$ given by eq 6, where M_L is the shift factor as defined as the molecular weight per unit contour length and M_0 is the molecular weight per repeat unit.

Comparison with the HW Theory. The equilibrium conformational behavior of the HW chain[4] may be described in terms of three model parameters: the constant differential geometrical curvature κ_0 and torsion τ_0 of its characteristic helix taken at the minimum zero of its elastic energy and the static stiffness parameter λ^{-1}. For a comparison of theory with experiment, the factor M_L introduced above is required to convert the total contour length L of the HW chain into the degree of polymerization x by the relation $L = xM_0/M_L$.

Now the mean-square optical anisotropy $\langle\Gamma^2\rangle$ of the HW chain of total contour length L (without excluded volume) may be written in the form[4,11]

$$\langle\Gamma^2\rangle = \lambda^{-1}L\sum_{j=0}^{2} C_j(\boldsymbol{\alpha},\ \kappa_0/\nu,\ \tau_0/\nu)\ f_j(\lambda L,\ \lambda^{-1}\nu) \tag{8}$$

where ν, C_j, and f_j are given by

$$\nu = (\kappa_0^{\,2} + \tau_0^{\,2})^{1/2} \tag{9}$$

$$C_0(\boldsymbol{\alpha},\ x,\ y) = \frac{1}{2}[2\alpha_{\zeta\zeta} - \alpha_{\xi\xi} - \alpha_{\eta\eta} - 3x^2(\alpha_{\zeta\zeta} - \alpha_{\eta\eta}) + 6xy\alpha_{\eta\zeta}]^2$$

$$C_1(\boldsymbol{\alpha},\ x,\ y) = 6[xy(\alpha_{\eta\eta} - \alpha_{\zeta\xi}) + (2y^2 - 1)\alpha_{\eta\zeta}]^2 + 6(x\alpha_{\xi\eta} + y\alpha_{\zeta\xi})^2$$

$$C_2(\boldsymbol{\alpha},\ x,\ y) = \frac{3}{2}(\alpha_{\xi\xi} - y^2\alpha_{\eta\eta} - x^2\alpha_{\zeta\zeta} + 2xy\alpha_{\eta\zeta})^2 + 6(y\alpha_{\xi\eta} + x\alpha_{\zeta\xi})^2 \tag{10}$$

$$f_j(x,\ y) = (j^2y^2 + 36)^{-2}\{6(j^2y^2 + 36) + (j^2y^2 - 36)x^{-1} + x^{-1}e^{-6x}[(36 - j^2y^2)\cos(jxy) - 12jy\sin(jxy)]\} \tag{11}$$

with α_{ij} ($i, j = \xi,\eta,\zeta$) being the ij component of the tensor $\boldsymbol{\alpha}$. It is convenient for the analysis of the experimental data to use the tensor $\boldsymbol{\alpha}_0$ instead of $\boldsymbol{\alpha}$. We then have from eqs 7 and 8

$$\langle\Gamma^2\rangle/x_w = (\lambda^{-1}M_L/M_0)\sum_{j=0}^{2} C_j(\boldsymbol{\alpha}_0,\ \kappa_0/\nu,\ \tau_0/\nu)\ f_j(\lambda L,\ \lambda^{-1}\nu) \tag{12}$$

where the reduced contour length λL is related to x_w by

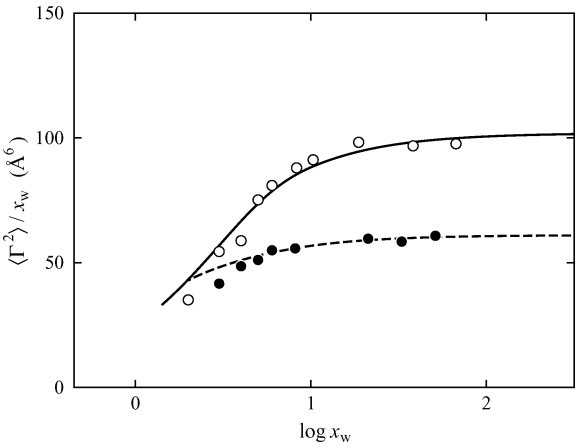

Figure 6. Plots of $\langle\Gamma^2\rangle/x_w$ against logx_w: (○) present data for a-PαMS in cyclohexane at 30.5 °C (Θ); (●) a-PS in cyclohexane at 34.5 °C (Θ).[7,8] The solid and dashed curves represent the HW theory values for a-PαMS and a-PS, respectively (see the text).

the equation

$$\log x_w = \log(\lambda L) + \log(\lambda^{-1}M_L/M_0) \tag{13}$$

The HW theory value of $\langle\Gamma^2\rangle/x_w$ as a function of x_w for a-PαMS may be calculated from eq 12 with eqs 6, 9−11, and 13 with the values of the HW model parameters previously determined from an analysis of $\langle S^2\rangle_\Theta$,[1] i.e., $\lambda^{-1}\kappa_0 = 3.0$, $\lambda^{-1}\tau_0 = 0.9$, $\lambda^{-1} = 46.8$ Å, and $M_L = 39.8$ Å^{-1}. The theoretical value of $\langle\Gamma^2\rangle/x_w$ in the limit of $x_w \to \infty$ may then be calculated to be 125 Å,[6] being somewhat larger than the experimental value 100 Å[6] given in the Results section. This slight overestimate of $\langle\Gamma^2\rangle$ may probably arise from the above-mentioned, rather simple calculation of $\boldsymbol{\alpha}_0$ in this case. In the following comparison between theory and experiment for the behavior of $\langle\Gamma^2\rangle/x_w$ as a function of x_w, therefore, we use $0.9_0\boldsymbol{\alpha}_0$ in place of $\boldsymbol{\alpha}_0$ itself in order to compensate for the theoretical overestimate. This modification of multiplying $\boldsymbol{\alpha}_0$ by the scalar factor 0.9_0 preserves the orientation of its principal axes with respect to the localized coordinate system mentioned in the last subsection, and does not affect the dependence itself of $\langle\Gamma^2\rangle/x_w$ on x_w. We note that the value of such a scalar factor previously used for a- and i-PMMAs[8,9] is 0.7_3, both of this value and the above one for a-PαMS being rather close to unity.

Figure 6 shows plots of $\langle\Gamma^2\rangle/x_w$ against logx_w for a-PαMS in cyclohexane at 30.5 °C (Θ). The unfilled circles represent the experimental values, and the solid curve the HW theory values so calculated. In the figure, the filled circles and the dashed curve represent the experimental and HW theory values, respectively, for a-PS in cyclohexane at 34.5 °C (Θ), which are discussed in the next subsection. Agreement between theory (with $0.9_0\boldsymbol{\alpha}_0$) and experiment for a-PαMS is satisfactory for $x_w \geq 5$, while the theoretical values are somewhat larger than the experimental ones for $x_w \leq 4$. This discrepancy for very small x_w may be regarded as arising from effects of chain ends that have not been taken into account in the HW theory.

Comparison with Other Polymers. First, we compare the present results for a-PαMS with the previous ones for a-PS in cyclohexane at 34.5 °C (Θ).[4,7,8] As mentioned above, the filled circles and the dashed curve in Figure 6 represent the experimental and HW theory values, respectively, for a-PS, which have been repro-

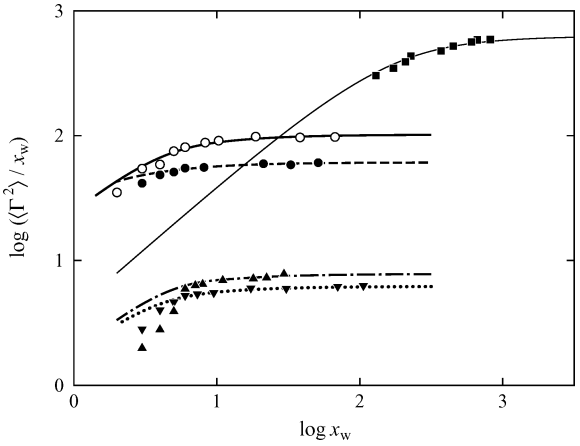

Figure 7. Double-logarithmic plots of $\langle\Gamma^2\rangle/x_w$ (in Å^6) against x_w: (○) present data for a-PαMS in cyclohexane at 30.5 °C (Θ); (●) a-PS in cyclohexane at 34.5 °C (Θ);[7,8] (▲) a-PMMA in acetonitrile at 44.0 °C (Θ);[8] (▼) i-PMMA in acetonitrile at 28.0 °C (Θ);[9] (■) PHIC in *n*-hexane at 25.0 °C.[10] The (heavy) solid, dashed, dot−dashed, dotted, and light solid curves represent the HW theory values for a-PαMS, a-PS, a-PMMA, i-PMMA, and PHIC, respectively (see the text).

duced from refs 7 and 8. The values of $\langle\Gamma^2\rangle/x_w$ for the two polymers for very small x_w are in rather good agreement with each other. As x_w is increased, $\langle\Gamma^2\rangle/x_w$ for a-PαMS increases more steeply than that for a-PS and approaches the asymptotic value 100 Å^6 appreciably larger than the value 61 Å^6 for a-PS.[8] Further, the value of x_w at which $\langle\Gamma^2\rangle/x_w$ reaches its asymptotic value is also somewhat larger for a-PαMS than for a-PS. Since the optical anisotropy of the α-methyl group is very small, the optical anisotropy of the repeat unit itself of PαMS may be considered to be almost identical to that of PS, as confirmed by the above-mentioned agreement in the range of very small x_w. The difference in the behavior of $\langle\Gamma^2\rangle/x_w$ for larger x_w between the two polymers may therefore be regarded as arising from those in chain stiffness and local chain conformation. It is clearly seen from the figure that the HW theory may explain satisfactorily that difference. It is important to note here that $\langle\Gamma^2\rangle/x_w$ is not directly related to the average dimension of polymer chains. In fact, the values of $\langle S^2\rangle_\Theta/x_w$ in the limit of $x_w\to\infty$ for a-PαMS[1] and a-PS[26] are 8.0_5 and 8.1_3 Å^2, respectively, and are almost identical to each other, while the asymptotic value of $\langle\Gamma^2\rangle/x_w$ for the former is about twice as large as that for the latter.

Next, we compare the results for a-PαMS and a-PS discussed above with those for a- and i-PMMAs[8,9] and PHIC.[10] Figure 7 shows double-logarithmic plots of $\langle\Gamma^2\rangle/x_w$ (in Å^6) against x_w. The unfilled and filled circles represent the above-mentioned values for a-PαMS and a-PS, and the filled triangles, inverted triangles, and squares represent the values previously obtained for a-PMMA in acetonitrile at 44.0 °C (Θ),[8] i-PMMA in acetonitrile at 28.0 °C (Θ),[9] and PHIC in *n*-hexane at 25.0 °C,[10] respectively. The (heavy) solid, dashed, dot-dashed, and dotted curves represent the HW theory values for a-PαMS, a-PS, and a- and i-PMMAs, respectively, and the light solid curve represents the KP theory values for PHIC. All the plots for a-PS, a- and i-PMMAs, and PHIC have been reproduced from Figure 6 of ref 10. It is interesting to see that $\langle\Gamma^2\rangle/x_w$ for each of the four flexible polymers reaches its asymptotic value at $x_w \simeq 10$, while that for PHIC reaches the corresponding value at much larger x_w ($\simeq 10^3$) because of its very large chain stiffness. We note that $\langle\Gamma^2\rangle/x_w$ for a- and i-PMMAs is very small compared to that for a-PαMS and a-PS since the optical anisotropy of the repeat unit of PMMA is very small compared to those for the latter two polymers.[8,9]

Conclusion

The mean-square optical anisotropy $\langle\Gamma^2\rangle$ has been determined for a-PαMS with $f_r = 0.72$ in cyclohexane at 30.5 °C (Θ) in the range of x_w from 2 to 67.1. It has been shown that the present values of $\langle\Gamma^2\rangle/x_w$ are much smaller than those obtained by Utiyama and Tsunashima,[15,16] and that the behavior of the former data is consistent with the existent theories. It has then been shown that the present results for $x_w \geq 5$ may be quantitatively reproduced by the HW theory values calculated with the values of the model parameters previously[1] determined from $\langle S^2\rangle_\Theta$ along with those of the local polarizability tensor $\boldsymbol{\alpha}_0$ of the repeat unit reasonably assigned. Thus, it is concluded that the HW theory may explain consistently the behavior of a variety of dilute solution properties $\langle\Gamma^2\rangle$, $\langle S^2\rangle$, $P_s(k)$, $[\eta]$, and D also for a-PαMS in the Θ state. From a comparison of the present data with the previous ones for a-PS,[4,7,8] a- and i-PMMAs,[4,8,9] and PHIC,[10] it has also been shown that the behavior of $\langle\Gamma^2\rangle$ depends remarkably on chain stiffness and local chain conformation, as was expected.

Acknowledgment. This research was supported in part by the 21st Century COE program COE for a United Approach to New Materials Science from the Ministry of Education, Culture, Sports, Science, and Technology, Japan.

References and Notes

(1) Osa, M.; Yoshizaki, T.; Yamakawa, H. *Macromolecules* **2000**, *33*, 4828.
(2) Ohgaru, Y.; Sumida, M.; Osa, M.; Yoshizaki, T.; Yamakawa, H. *Macromolecules* **2000**, *33*, 9316.
(3) Suda, I.; Tominaga, Y.; Osa, M.; Yoshizaki, T.; Yamakawa, H. *Macromolecules* **2000**, *33*, 9322.
(4) Yamakawa, H. *Helical Wormlike Chains in Polymer Solutions*; Springer: Berlin, 1997.
(5) Tamai, Y.; Konishi, T.; Einaga, Y.; Fujii, M.; Yamakawa, H. *Macromolecules* **1990**, *23*, 4067.
(6) Patterson, G. D.; Flory, P. J. *J. Chem. Soc., Faraday Trans. 2* **1972**, *68*, 1098 and succeeding papers.
(7) Konishi, T.; Yoshizaki, T.; Shimada, J.; Yamakawa, H. *Macromolecules* **1989**, *22*, 1921.
(8) Takaeda, Y.; Yoshizaki, T.; Yamakawa, H. *Macromolecules* **1993**, *26*, 3742.
(9) Takaeda, Y.; Yoshizaki, T.; Yamakawa, H. *Macromolecules* **1995**, *28*, 4167.
(10) Nakatsuji, M.; Ogata, Y.; Osa, M.; Yoshizaki, T.; Yamakawa, H. *Macromolecules* **2001**, *34*, 8512.
(11) Yamakawa, H.; Fujii, M.; Shimada, J. *J. Chem. Phys.* **1979**, *71*, 1611.
(12) Nagai, K. *Polym. J.* **1972**, *3*, 67.
(13) Arpin, M.; Strazielle, C.; Weill, G.; Benoit, H. *Polymer* **1977**, *18*, 262.
(14) Kratky, O.; Porod, G. *Recl. Trav. Chim. Pays−Bas* **1949**, *68*, 1106.
(15) Utiyama, H.; Tsunashima, Y. *J. Chem. Phys.* **1972**, *56*, 1626.
(16) Tsunashima, Y. Ph.D. Thesis, Kyoto University, 1972.
(17) Osa, M.; Sumida, M.; Yoshizaki, T.; Yamakawa, H.; Ute, K.; Kitayama, T.; Hatada, K. *Polym. J.* **2000**, *32*, 361.
(18) Hermans, J. J.; Levinson, S. *J. Opt. Soc. Am.* **1951**, *41*, 460.
(19) (a) Utiyama, H.; Kurata, M. *Bull. Inst. Chem. Res. Kyoto Univ.* **1964**, *42*, 128. (b) Utiyama, H. *J. Phys. Chem.* **1965**, *69*, 4138.
(20) Fujii, M.; Nagasaka, K.; Shimada, J.; Yamakawa, H. *Macromolecules* **1983**, *16*, 1613.

(21) Flory, P. J. *Statistical Mechanics of Chain Molecules*; Interscience: New York, 1969.
(22) Flory, P. J.; Sundararajan, P. R.; DeBolt, L. C. *J. Am. Chem. Soc.* **1974**, *96*, 5015.
(23) Sundararajan, P. R. *Macromolecules* **1977**, *10*, 623.
(24) Patterson, G. D.; Flory, P. J. *J. Chem. Soc., Faraday Trans. 2* **1972**, *68*, 1111.
(25) Suter, U. W.; Flory, P. J. *J. Chem. Soc., Faraday Trans. 2* **1977**, *73*, 1521.
(26) Abe, F.; Einaga, Y.; Yoshizaki, T.; Yamakawa, H. *Macromolecules* **1993**, *26*, 1884.

MA034536R